UC Santa Cruz
UC Santa Cruz Previously Published Works

Title

Î²-Cyclodextrin at the water/1-bromobutane interface: molecular insight into reverse phase transfer catalysis

Permalink

Authors

Chief Elk, Jackson
Benjamin, Ilan

Publication Date

2015-04-24

DOI

Peer reviewed

β−Cyclodextrin at the water/1-bromobutane interface: molecular insight into reverse phase transfer catalysis

Jackson Chief Elk and Ilan Benjamin*
Department of Chemistry and Biochemistry
*University of California Santa Cruz, CA 95064*

Abstract:

Molecular insight into the role of β-cyclodextrin (βCD) as a phase transfer catalyst at the liquid/liquid interface is obtained by molecular dynamics simulations of the structure and dynamics of β-cyclodextrin (βCD) adsorbed at the interface between water and 1-bromobutane. In particular, we consider the structure and dynamics of the water and bromobutane molecules inside the βCD cavity and compare them with the behavior when βCD is dissolved in bulk water. βCD is preferentially oriented at the interface, with the cavity opening along the interface normal. While in bulk water the cavity includes 6-8 water molecules that are relatively mobile with short residence time, at the interface the cavity is mostly dehydrated and includes a single bromobutane molecule. This inclusion complex is stable in bulk water. The implication of this behavior for reverse phase transfer catalysis is discussed.

*Email: benjamin@chemistry.ucsc.edu , Telephone: 831-459-3152

I. INTRODUCTION

There is considerable interest in the use of cyclodextrins (CD) as hosts for carrying out chemical reactions in solution for a variety of applications.[1-3] The interior of these cyclic oligosaccharide/polyalcohols, made of n D-glucose monomers (n = 6-9), consists of a hydrophobic ring of C-H groups. It enables the stabilization of a hydrophobic reactant in water, while the exterior hydroxyl groups make the CDs somewhat soluble in water (0.016M at 298K for βCD with n = 7). Specifically, βCD is a distorted, cylindrically shaped object (internal diameter about 0.7nm), with one opening slightly larger than the other. (See Fig. 1)
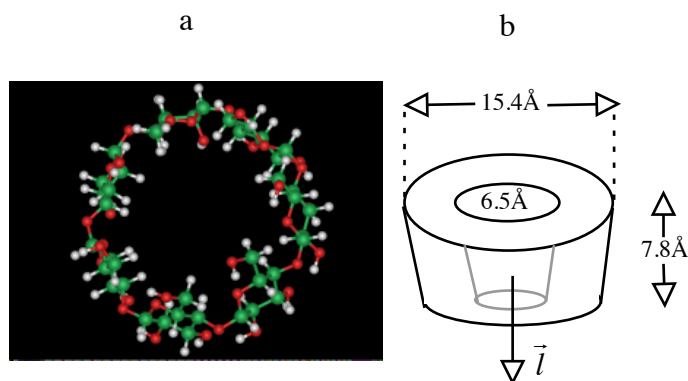
Fig. 1. The molecular structure (a) and the dimensions (b) of the β-cyclodextrin molecule.

A specific application of CDs, which is related to the topic of this work, is their increased usage as inverse phase transfer catalysts (IPTC).[4-9] In this case, a hydrophobic reagent is transferred from the organic phase to the aqueous phase across the

water/organic liquid interface, and the reaction takes place either in bulk water or at the aqueous-side of the interface. This is essentially the reverse process of using crown ethers as normal phase transfer catalysts, a process which has received more attention.[10-11] The use of CDs as IPTC at the liquid/water interface provides exciting new opportunities for "green" organic synthesis, while also raising fundamental questions in the areas of heterogeneous catalysis, host-guest chemistry and reactions in confined geometries. For example, βCD has been used as an IPTC in the S_N2 reaction of 1-bromo-octane with CN^-, I^- and SCN^- at the water/1-bromo-alkane interface.[12] The reaction rate was significantly enhanced relative to the rate at the interface without the catalyst, and was much faster than when αCD ($n = 6$) is used. However, the rate is slower than when the reaction takes place with a quaternary ammonium ion catalyst (in the organic phase). It has been suggested that the water hydration of the nucleophile plays a role in slowing this reaction down, but it is unclear whether this is water that resides inside or outside the cavity. Other examples of reactions studied under conditions of IPTC include the hydroformylation of olefins,[13] Wacker oxidation of olefins,[14] the hydrogenation of aldehydes[15], and the isomerization reaction of 4-allylanisole.[16]

X-ray studies of βCD crystals and the molecular dynamics simulations of aqueous solutions of βCD show that some water molecules (possibly as many as 7) are located inside the cavity.[17-19] These water molecules will influence the binding of the substrate to the cavity, since all or some must be released to enable binding. If any water molecules remain while the guest molecule is in the cavity, they are likely to influence the reaction rate in a way similar to the retarding effect of water on the nucleophilic attack carried out

in bulk organic solvents.[20] Indeed, a recent MD study suggests an effective dielectric constant in the range of 3-8 for the cavity, depending on the probe's orientation.[21] Several molecular dynamics simulations of inclusion complexes (in homogeneous solutions) have been published, shedding further light on the nature of the cavity.[22-27]

As a preliminary step for understanding the role of βCD as an IPTC, it is important to characterize its behavior at the liquid/liquid interface and, in particular, the interplay between water and the organic solvent structure and dynamics at the liquid/liquid interface. While αCD and βCD are not surface-active at the air/water interface, they form surfactants as inclusion complexes with linear oil molecules at the oil-water interface, as was recently demonstrated experimentally.[28] Molecular dynamics studies of βCD at the water/chloroform and the water/liquid hydrocarbon interfaces[22-23] suggest that despite its solubility in water, βCD strongly adsorbs at the interface and that this adsorption is key to its catalytic activity in the two-phase hydroformylation reaction of olefins. Since the interior of the cavity is hydrophobic, there is a competition between the hydrophobic substrate and the organic solvent molecules to enter the cavity, and the simulations indeed observed one chloroform molecule inside the cavity complex at the water/chloroform interface.[22] Furthermore, a key step in the ability of βCD to catalyze a reaction is its acting as a receptor for a hydrophobic reactant that is residing in the organic phase. The complex can then be transferred to the bulk aqueous phase, where it can react with a hydrophilic reactant. (If the hydrophilic reactant has an appreciable surface concentration, the reaction can take place at the interface). The abovementioned simulations show no strong orientational preference regarding the opening of the cavity,

but clearly the instantaneous orientation coupled with normal density fluctuations at the interface must be important for a successful insertion of the reactant. Of course, the size of the reactant in relation to the size of the cavity is of prime importance, but in addition, because no covalent bonds are formed or broken in this process, one possible driving force is the release of water molecules from the low polarity cavity to the outside pool, where they can form new hydrogen bonds. This process could also be coupled to surface water fluctuations.

In order to gain molecular insight into these processes, we consider in this paper the structure and dynamics of βCD adsorbed at the interface between water and 1-bromobutane (BrBut). The choice of BrBut is motivated by the important feature of the experimental system in which the solvent is acting as a substrate for an S_N2 reaction with a suitable nucleophile (to be considered in future work). We pay particular attention to the structure and dynamics of the water and BrBut molecules inside the βCD cavity and compare them with the behavior when βCD is in bulk water.

The rest of the paper is organized as follows. In section II, we describe the systems studied and the methodology used. In section III, we describe and discuss the results, followed by conclusions in section IV.

II. SYSTEMS AND METHODS

MD simulations were performed using version 4.54 of GROMACS.[29] The simulation box consists of one βCD, 4559 water molecules and 793 1-bromobutane

(BrBut) molecules in a box of dimension 5.43 nm x 5.43 nm x10.80 nm. Periodic boundary conditions are applied in all directions resulting in two liquid/liquid interfaces near Z = 5.25 nm and near Z = 0. The temperature and the pressure are held constant at 298.15 K and 1 atm utilizing the V-rescale thermostat (coupling constant of 0.1 ps) and Parrinello– Rahman barostat (coupling constant of 2 ps). The equations of motion are integrated using the leapfrog algorithm with a time step of 2 fs. The smooth version of the particle mesh Ewald (PME) is used to treat the long-range electrostatics (grid spacing of 0.16 PME order of 4, real-space cutoff of 1nm).

The bonded and nonbonded βCD force field parameters were previously derived to be consistent with the AMBER99SB-ILDN force field.[30] A rigid TIP3P water model was used. For BrBut, bonded and nonbonded terms were generated using the python program ACPYE[31], and further partial charge optimizations were performed using the Yasara AutoSMILES server.[32-33] The alkane parameters were tested at liquid/liquid interfaces by Brooks and co-workers[34]. The simulated bulk density of BrBut in contact with water agrees very well with the experimental value (see below).

The intermolecular potential energy functions used here are pair-wise additive, with the polarizable nature of the solvent and the βCD being effectively included by the proper adjustment of the Lennard-Jones parameters and the point charges. While many-body polarizable effects have been shown to be important for ions at hydrophobic interfaces[35-38] and could be important here as well, they are unlikely to significantly alter our main conclusions.

The βCD is inserted near Z = 5 nm, and the system is equilibrated for 600 ps, followed by a 73 ns trajectory with all atomic configurations saved every 0.5 ps. As a reference, a 50 ns simulation was also performed of a single βCD in bulk water using 1285 water molecules in a cubic box of size 3.43^3 nm. An additional 50 ns simulation of an inclusion complex made of a single BrBut molecule inside the βCD cavity in bulk water was carried out, as will be discussed below. The saved configurations from these simulations were used to compute structural and dynamical information, as detailed below. The calculation of water molecules' orientational correlation functions requires shorter spaced configurations, and for this a 1 ns trajectory, where configurations are saved every 5 fs (using an integration time step of 1 fs), was also run.

III. RESULTS AND DISCUSSION

The density profiles of water (oxygen site) and the BrBut center of mass, together with the probability distribution of the βCD center of mass, are shown in Fig. 2. The Gibbs dividing surface (where the water density is approximately 50% of the bulk value) is near Z = 5 nm. The βCD center of mass' probability distribution reflects the observation that this solute remains adsorbed at the liquid/liquid interface for the duration of the 73 ns trajectory and is thus consistent with the assumption that despite its solubility in water, it is surface active. During the simulation, the βCD samples the entire 1.5 nm width of the interface, while freely moving in the plane parallel to the interface, sampling the full width of the lamella (see supplementary Fig. S1). The presence of βCD at the interface slightly increases its width. This can be inferred by comparing the density

profile of water at the two liquid/liquid interfaces in the simulation box (see supplementary Fig. S2).
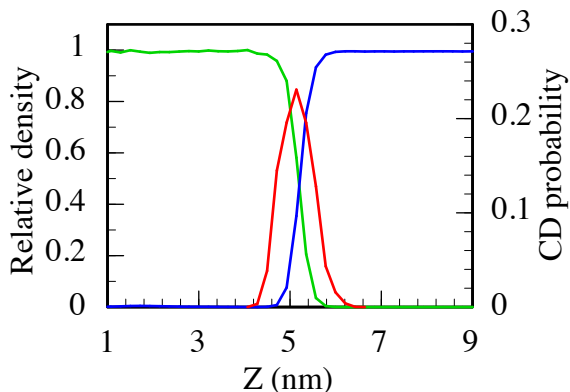
Fig. 2. Density profiles (relative to bulk solvent density, left axis) of water oxygen (blue line), BrBut center of mass (green line), and the probability distribution of the βCD center of mass (red line, right axis).

Since our focus is on the cavity region of βCD, in order to clearly define this region, we show in Fig. 3 the water (O)-βCD (center of mass) radial distribution function when the βCD is at the liquid/liquid interface and in bulk water. In bulk water, the peak near 0.2 nm represents water molecules trapped in the cavity. The peak is shifted away from the r = 0 central position by 0.2 nm, which is in agreement with neutron-diffraction studies.[39] This suggests that the water molecules are more likely to wet the inside walls of the cavity, rather than accumulate in the center. The tail beginning at 0.4 nm and continuing with the plateau up to about 0.6 nm represents, in part, water molecules at both mouths of the cylindrically shaped cavity. The peak near 0.9 nm represents water molecules

hydrating the OH groups on the outside of βCD, with a second hydration shell near 1.2 nm. The integral of the radial density:

$$n(r) = 4\pi\rho_{BW} \int_0^r x^2 g(x) dx \qquad , \qquad (1)$$

where $\rho_{BW} = 33.43$ nm^{-3} is the density of bulk water at 298K, gives the number of water molecules between 0 and r and is shown as a red line (corresponding values on the right axis). This integral indicates that if we define the cavity region to be the sphere centered at zero that reaches up to but does not include the water molecules at the mouth of the cavity, then there are 7 water molecules inside the cavity. This value is in reasonable agreement with experimental data[40-42] and other simulations.[43-44] For example, Cezard *et al* have compared the performance of several force fields for the structure of several CDs and their derivatives in water.[18] Depending on the choice of force fields, the number of water molecules inside the cavity ranges from 6.5 to 8.2. Their q4MD-CD force field seems to offer the best agreement with experimental data and with the results reported here.
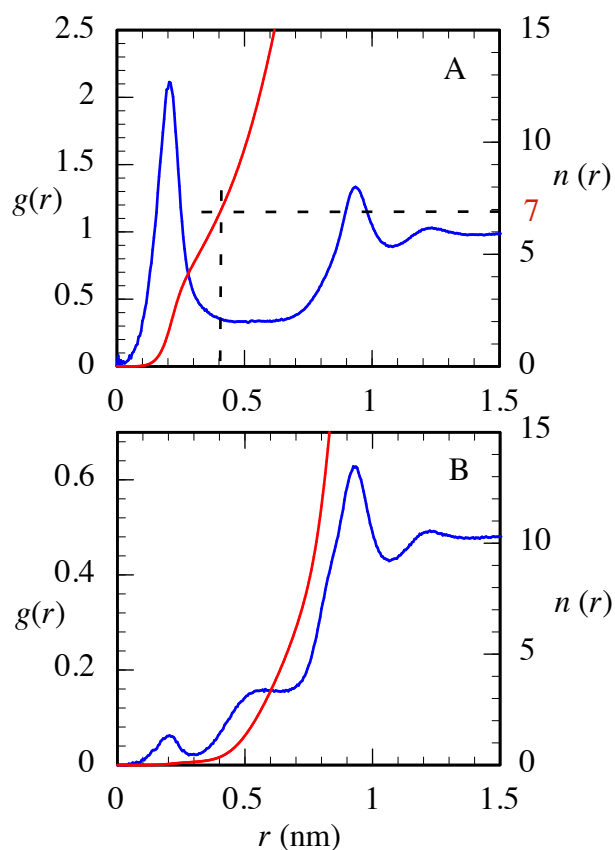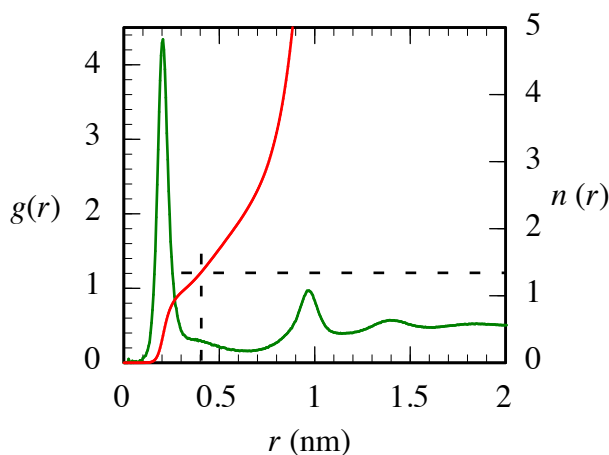
Fig. 3. Water(O)-βCD center of mass radial distribution function in bulk water (A) and at the water/BrBut interface (B). The red lines correspond to the integrated number of water molecules (right axis).

Panel B shows the corresponding results when the βCD is adsorbed at the water/BrBut interface from the 73 ns simulation. While the main features observed in the bulk (peak at 0.2 nm, the plateau region and peaks at 0.9 nm and 1.2 nm) are present here, their magnitude is much reduced. The integrated density shown in red suggests that the cavity is occupied on average by only 0.35 water molecules (or one water molecule

during an average total 1/3 of the simulation time). Note also that the asymptotic value $g(r > 1.5 \text{ nm}) \approx 0.5$ reflects the fact that the center of mass of βCD is near the Gibbs dividing surface, so approximately 50% of a spherical shell (with radius > 1.5 nm) centered at the βCD center of mass contains water molecules.

Fig. 4 shows the radial distribution function calculated between the Br atom of BrBut and the center of mass of βCD. Our focus on the Br atom of the molecule is due to the fact that this is the reaction center of interest. In the absence of water molecules, using the above definition of the cavity region of βCD, this region is occupied by an average of 1.33 BrBut molecules. This number is slightly greater than the number one expects from the relative size of the water and the BrBut solvent: $\rho_{\text{W}}/\rho_{\text{BrB}} = 33.4 \text{nm}^{-3}/5.58 \text{nm}^{-3} = 6.0$ (which gives 7.0/6.0 = 1.17 BrBut molecules). This represents the affinity of the hydrophobic cavity of βCD to the hydrophobic solvent and is consistent with the relatively sharp peak near 0.2 nm.

Fig. 4. Brombutane(BrBut)-βCD center of mass radial distribution function at the water/BrBut interface. The red line corresponds to the integrated number of BrBut molecules (right axis).

A different perspective regarding the composition of the βCD cavity is provided in Fig. 5. This figure shows that the content of the cavity region experiences large fluctuations. While the cavity includes on average 7 water molecules when βCD is in bulk water, there is a significant probability of having 6 or 8 water molecules present in the cavity. When βCD is at the interface, the cavity is mostly empty of water, but there is a non-negligible probability of finding one water molecule inside the cavity. The probability of finding up to 7 water molecules inside the cavity is not strictly zero. On the other hand, there is a significant probability of finding one or two BrBut molecules inside the cavity when βCD is at the interface (bottom left panel). The two-dimensional joint probability distribution (bottom right panel) shows that one water molecule is more likely (P = 0.1) to be found inside the cavity if it is simultaneously occupied by one BrBut molecule than when there are no BrBut molecules (P< 0.01). This is due to the single water association with the Br atom, but it must be stressed that the probability that the cavity is empty is P < 0.001. Thus, when βCD is adsorbed at the liquid/liquid interface, the water content is nearly fully replaced by the organic solvent, in contrast with the 50% distribution of the surrounding medium, reflecting the hydrophobic nature of the cavity. This has an important implication for the ability of βCD to serve as a carrier for a hydrophobic substrate for a nucleophilic attack by a water-soluble nucleophile. The

association of a single water molecule with the Br atom in the cavity can have implications for lowering the rate of a nucleophilic attack.
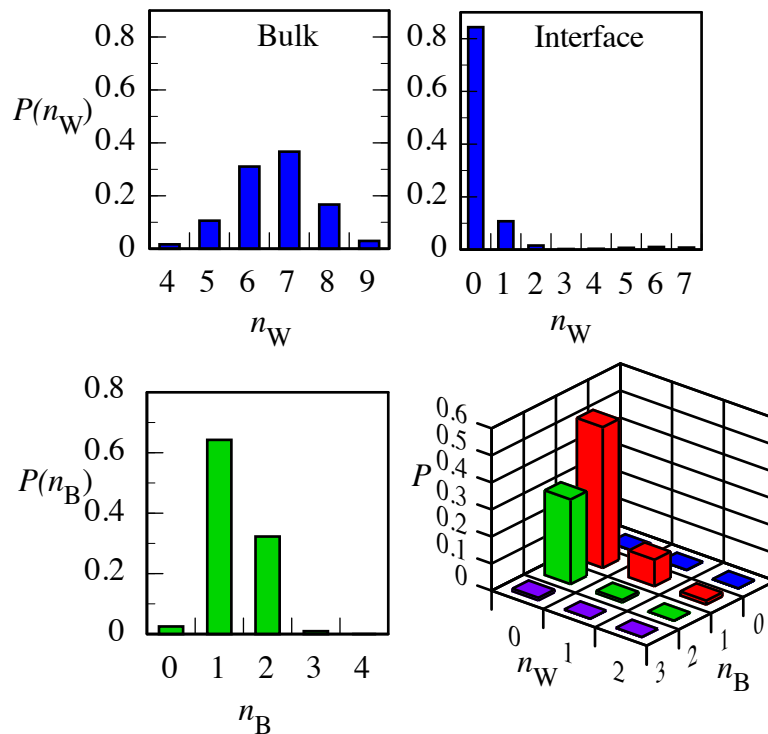
Fig. 5. Top panels: Probability histograms of finding n_W water molecules inside the βCD cavity region when βCD is dissolved in bulk water (left) and when the βCD is at the water/BrBut interface (right panel). Bottom left: Probability histograms of finding n_B BrBut molecules inside the βCD cavity region. Bottom right: Joint probability histogram of simultaneously finding n_W water molecules and n_B BrBut molecules inside the cavity.

Interestingly, a similar affinity for the (somewhat) hydrophobic solvent was observed by Laria and coworkers for βCD in water/DMSO 50:50 mixtures.[45] Because of a different definition of the cavity region (cylindrical with 20% smaller volume than our definition),

the cavity contains on average 5 water molecules when the βCD is in bulk water and 1 DMSO molecule when in bulk DMSO. In the 50:50 mixture, the cavity contains mostly one DMSO molecule (probability = 0.7) and infrequently 1 water molecule (probability = 0.2).

The dynamics of solvent exchange between the cavity and the surrounding medium can be examined by calculating the residence time correlation function. We define a dynamical variable $h_i(t) = 1$ when a solvent molecule "i" is inside the cavity at time t, given that it was inside the cavity at $t = 0$. The residence time correlation function $C(t)$ is defined as the equilibrium time correlation function:

$$C(t) = \frac{1}{N} \sum_{i=1}^{N} \frac{\langle h_i(t)h_i(0) \rangle}{\langle h_i(0)h_i(0) \rangle} \quad , \quad (2)$$

where the sum is over all the solvent molecules, and the ensemble average is over all time origins. A plot of Eq. 2 for βCD in bulk water and at the interface is given in Fig. 6. This figure shows that when βCD is in bulk water, the cavity's water molecules exchange quite rapidly with surrounding water molecules, with an average decay time of $C(t)$ about 50 ps. Dielectric relaxation measurements give an exchange rate of 20-25 ps.[46] A time delay τ can be introduced into the definition of the residence time correlation function to avoid counting molecules that have exited for a time period smaller than τ. An increase in τ increases the residence time because molecules that reenter the cavity within this time period are considered to have never left. Our average residence time is in

14

reasonable agreement with that of Cezard et al[18] and of Rodriguez et al.[45] Tidemand et al[19] calculated much shorter residence time (7.8 ps), but their cavity is defined to be a sphere of radius 0.5 nm, which corresponds to a larger water pool (10 water molecules), so it is probable that their rate is dominated by rapid movement of water molecules near the mouth of the cavity. It is interesting to note that the average time for a TIP3P water molecule to diffuse ($D = 6 \times 10^{-3}$ nm^2/ps) across the 0.8 nm cavity (from one mouth to the opposite, along the diameter of our spherically defined cavity) is $l^2 / 2D \approx 53$ ps. However, a significant number of trajectories that contribute to the relaxation of $C(t)$ involve water molecules that rapidly exchange across one end of the cavity. If we chose τ = 10 ps, our average relaxation time increases to 75 ps, likely representing trajectories that transverse the cavity and thus correspond to a slower than bulk diffusion process.

When βCD is at the interface, the much smaller water content of the cavity (mostly just a single water molecule) is longer-lived (180 ps) while the one or two BrBut molecules are much longer-lived. A short transient (reflecting a small percentage of molecules leaving and reentering at the mouth of the cavity) is followed by a very slow exponential decay with a time constant of 3 ns. The slow exchange of BrBut compared with the more rapid water exchange suggests a relatively stable inclusion complex that can live long enough to allow for an attacking nucleophile to complete a reaction.
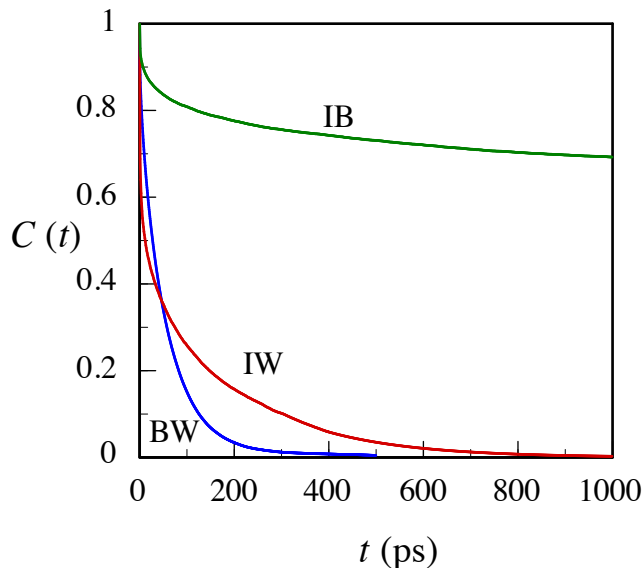
Fig. 6. Water cavity residence time correlation functions (Eq. 2). The lines labeled BW, IW are for water molecules when βCD is in bulk water and at the interface, respectively. The line labeled IB is for BrBut residence when the βCD is at the interface.

As the βCD diffuses away from the interface and carries the single BrBut molecule, it is interesting to consider the stability of this complex. We have performed a separate 50ns-simulation of βCD with a single BrBut in its cavity. As shown in Fig. 7, the BrBut remained inside the cavity for the entire 50ns-trajectory. Unlike the situation at the interface, there is a significant probability that the cavity also has water molecules co-existing with the single BrBut molecule. We find that the cavity includes 0, 1, 2 or 3 water molecules with probabilities $0.41, 0.36, 0.16$ and 0.06, respectively.
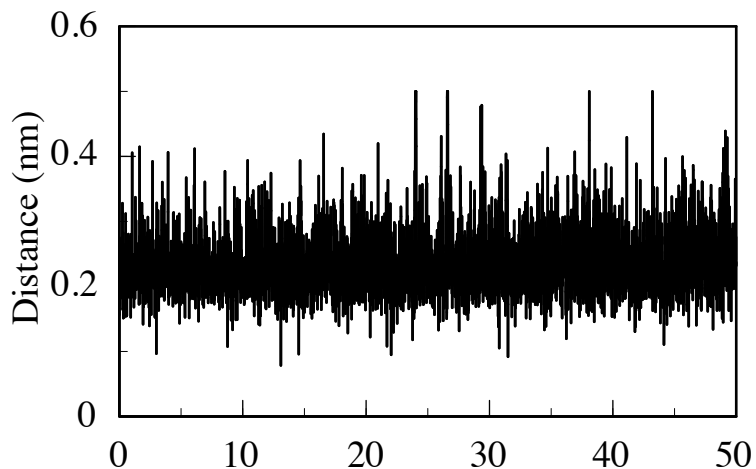
Fig. 7. The distance between the Br atom of BrBut and the center of the βCD cavity during a 50 ns trajectory of an inclusion complex in bulk water.

Since a key condition for the ability of BrBut to enter the βCD cavity is the mobility of water molecules, it is interesting to examine the rotational dynamics of the water molecules in the cavity. Let $\mathbf{d}_i(t)$ be the unit vector along the electric dipole of the i'th water molecule at time t. We define the single molecule dipole autocorrelation function $C_w(t)$ for water molecules in the cavity of βCD as follows:

$$C_w(t) = \frac{1}{N} \sum_{i=1}^{N} \langle \mathbf{d}_i(t) \cdot \mathbf{d}_i(0) \rangle \quad , \tag{3}$$

where the sum is over all the water molecules that remain in the cavity during the time period t, and the ensemble average is over all time origins. Fig. 8 compares the water dipole autocorrelation function for cavity water molecules and for bulk water (far away

from the βCD). We find that the cavity water average reorientation time (defined as

$\int_0^\infty C_w(t)dt$) is 7.5 ps compared with 2.3 ps for bulk water. These results are similar to

those found for water near hydrophobic surfaces and in the interior of micelles.[47] The

slowing down of water molecules inside a hydrophobic cavity can be explained using the

jump mechanism suggested by Laage and Hynes.[48] In this mechanism, bulk water

reorientation follows concertedly with the breaking of a hydrogen bond with an over-

coordinated first-shell neighbor to form a hydrogen bond with a second-shell water

molecule. Inside a hydrophobic cavity, where only a few water molecules are available to

form a hydrogen bond, the extra stability of this bond and the lack of available neighbors

make the reorientation dynamics slower.
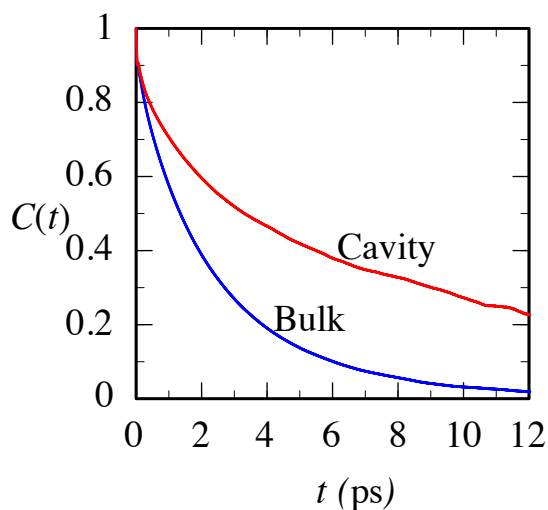
Fig. 8. Water molecule dipole time rotational correlation function for water molecules in the cavity of βCD (red line) compared with bulk water (blue line).

Clearly, for the BrBut to enter the cavity while the βCD is adsorbed at the interface, the orientation of the main axis along the cylindrical cavity with respect to the interface and the reorientation dynamics of this vector are of interest. Denoting by $\vec{l}$ the unit vector in this direction (defined using the normal to the plane made of three oxygen atoms, see supplementary Fig. S3), Fig. 9 shows the probability distribution of cosθ, where θ is the angle between $\vec{l}$ and the normal to the interface, calculated in different 0.2 nm-wide slabs parallel to the interface. This figure shows that the βCD is oriented with the opening of the cavity pointing towards the interface (either the narrow or the wide ends with nearly equal probabilities). The orientational preference is largely gone when the βCD's center of mass is about 0.6 nm away from the Gibbs surface.
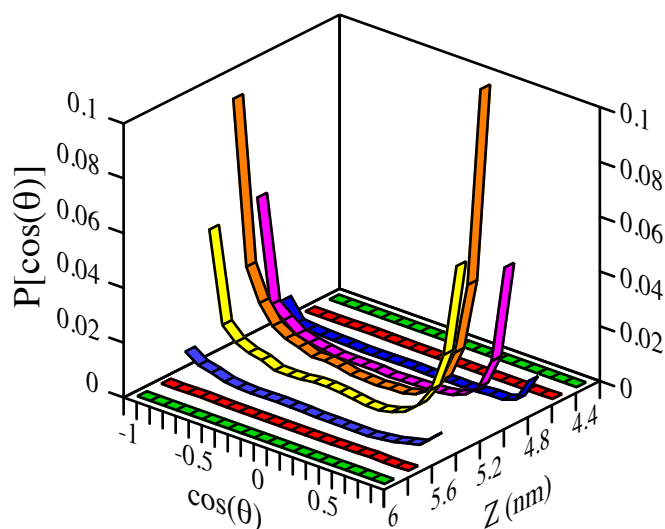

Fig. 9. Probability distributions for the cosine angle between the main axis of βCD and the normal to the water-BrBut interface in different slabs. The Gibbs surface is at 5.0 nm.

Fig. 10 shows the equilibrium time correlation function (of course, $\vec{l}(0)\cdot\vec{l}(0)=1$)

$$C_i(t) = \langle \vec{l}(t) \cdot \vec{l}(0) \rangle \qquad , \qquad (4)$$

calculated using the entire 73 ns trajectory. The βCD exhibits reorientation dynamics on two time scales: the wobbling of the main axis is responsible for the initial relatively rapid ≈80 ps decay, followed by the slower diffusion of the main axis with a ≈1.3 ns time constant. This is slower than the reorientation dynamics in the bulk, where the two components are ≈35 ps and ≈300 ps. Since the surface reorientation time is significantly slower than the time scale for the BrBut to diffuse the few tenths of a nm required to enter the cavity, we conclude that structural and dynamical considerations promote the easy insertion of the BrBut molecules into the cavity.
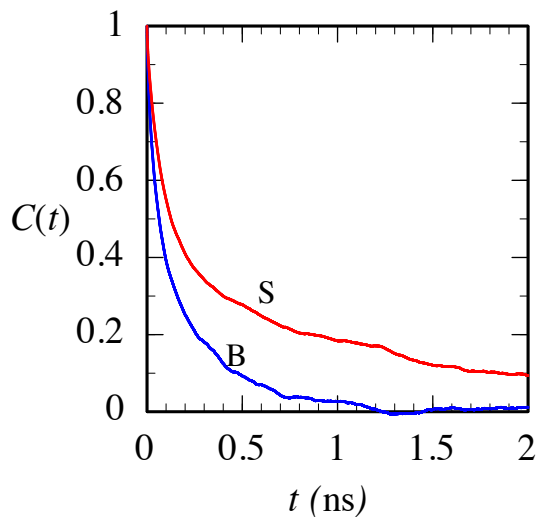
Fig. 10. Equilibrium reorientational time correlation function of the main axis of βCD at the water-BrBut interface (red line, labeled S) compared with that in bulk water (blue line, labeled B). (Eq. 4)

20

IV. CONCLUSIONS

Our simulations show that βCD is adsorbed at the water /1-bromobutane interface and oriented with the opening of the cavity along the interface normal. In bulk water, the cavity includes 6-8 water molecules with a short residence time (50 ps), in good agreement with experiments. At the interface, the cavity most likely includes a single bromobutane molecule with a relatively long residence time (3 ns) and no appreciable water molecules. This inclusion complex is stable in bulk water on the 50 ns time scale, but has a 60% chance of simultaneously including 1-3 water molecules. These results suggest that βCD could act as a reverse phase transfer catalyst for accelerating a nucleophilic attack in bulk water, but the rate may be lower (than in bulk organic liquid) due to the co-existence of water molecules in the cavity.

Supporting Information Available

Figs. S1-S3. This information is available free of charge via the Internet at http://pubs.acs.org/.

References

(1) Takahashi, K., Organic Reactions Mediated by Cyclodextrins. *Chem. Rev.* **1998,** *98*, 2013-2033.

(2) Easton, C. J., Cyclodextrin-Based Catalysts and Molecular Reactors. *Pure Appl. Chem.* **2005,** *77*, 1865-1871.

(3) Mukhopadhyay, M.; Banerjee, D.; Mukherjee, S., Proton-Transfer Reaction of 4-Methyl 2,6-Diformyl Phenol in Cyclodextrin Nanocage. *J. Phys. Chem. A* **2006,** *110*, 12743-12751.

(4) Mathias, L. J.; Vaidya, R. A., Inverse Phase-Transfer Catalysis - 1st Report of a New Class of Interfacial Reactions. *J. Am. Chem. Soc.* **1986,** *108*, 1093-1094.

(5) Fife, W. K.; Xin, Y., Inverse Phase-Transfer Catalysis - Probing Its Mechanism with Competitive Transacylation. *J. Am. Chem. Soc.* **1987,** *109*, 1278-1279.

(6) Shimizu, S.; Sasaki, Y.; Hirai, C., Inverse Phase-Transfer Catalysis by Cyclodextrins - Palladium-Catalyzed Reduction of Bromoanisoles with Sodium Formate. *Bull. Chem. Soc. Japan* **1990,** *63*, 176-178.

(7) Boyer, B.; Hambardzoumian, A.; Roque, J. P.; Beylerian, N., Reaction in Biphasic Water/Organic Solvent System in the Presence of Surfactant: Inverse Phase Transfer Catalysis Versus Interfacial Catalysis. *Tetrahedron* **2000,** *56*, 303-307.

(8) Lu, Y. L.; Jwo, J. J., Inverse Phase Transfer Catalysis: Kinetics of the Pyridine-1-Oxide-Catalyzed Two-Phase Reactions of Methyl-, Methoxy-, Iodo-, and Nitro-Benzoyl Chlorides and Benzoate Ions. *J. Mol. Catal. A-Chem.* **2001,** *170*, 57-65.

(9) Boyer, B.; Hambardzoumian, A.; Roque, J. P.; Beylerian, N., Inverse Phase Transfer Catalysis Versus Interfacial Catalysis. Effect of Medium Stirring in the Epoxidation Reaction of Chalcone by Hydrogen Peroxide. *J. Chem. Soc.-Perkin Trans. 2* **2002**, 1689-1691.

(10) Baudoul, F.; Borcy, A.; Mommerency, S.; Vanderwegen, P.; Jannes, G., The Influence of Water on Cyanide Displacement of 1-Halobutanes Using 18-Crown-6 Ether as Phase Transfer Catalyst. *J. Mol. Catal A-Chem.* **1996,** *107*, 351-358.

(11) Volkov, A. G., *Interfacial Catalysis*. Marcel Dekker: New York, 2003.

(12) Trifonov, A. Z.; Nikiforov, T. T., Cyclodextrins as Phase-Transfer Catalysts in a Nucleophilic Displacement Reaction. *J. Mol. Catal.* **1984,** *24*, 15-18.

(13) Monflier, E.; Fremy, G.; Castanet, Y.; Mortreux, A., Molecular Recognition between Chemically-Modified Beta-Cyclodextrin and Dec-1-Ene - New Prospects for Biphasic Hydroformylation of Water-Insoluble Olefins. *Angew. Chem. Int. Ed. Engl.* **1995,** *34*, 2269-2271.

(14) Monflier, E.; Tilloy, S.; Blouet, E.; Barbaux, Y.; Mortreux, A., Wacker Oxidation of Various Olefins in the Presence of Per(2,6-Di-O-Methyl)-Beta-Cyclodextrin: Mechanistic Investigations of a Multistep Catalysis in a Solvent-Free Two-Phase System. *J. Mol. Catal. A -Chem.* **1996,** *109*, 27-35.

(15) Monflier, E.; Tilloy, S.; Castanet, Y.; Mortreux, A., Chemically Modified Beta-Cyclodextrins: Efficient Supramolecular Carriers for the Biphasic Hydrogenation of Water-Insoluble Aldehydes. *Tetrahedron Lett.* **1998,** *39*, 2959-2960.

(16) Jwo, J.-J., Phase Transfer Catalysis: Fundamentals and Selected Systems. In *Interfacial Catalysis*, Volkov, A. G., Ed. Marcel Dekker: New York, 2003; pp 227-284.

(17) Lawtrakul, L.; Viernstein, H.; Wolschann, P., Molecular Dynamics Simulations of Beta-Cyclodextrin in Aqueous Solution. *Int. J. Pharm.* **2003,** *256*, 33-41.

(18) Cezard, C.; Trivelli, X.; Aubry, F.; Djedaini-Pilard, F.; Dupradeau, F. Y., Molecular Dynamics Studies of Native and Substituted Cyclodextrins in Different Media: 1. Charge Derivation and Force Field Performances. *Phys. Chem. Chem. Phys.* **2011,** *13*, 15103-15121.

(19) Tidemand, K. D.; Schonbeck, C.; Holm, R.; Westh, P.; Peters, G. H., Computational Investigation of Enthalpy-Entropy Compensation in Complexation of Glycoconjugated Bile Salts with Beta-Cyclodextrin and Analogs. *J. Phys. Chem. B* **2014,** *118*, 10889-10897.

(20) Albanese, D.; Landini, D.; Maia, A.; Penso, M., Key Role of Water for Nucleophilic Substitutions in Phase-Transfer-Catalyzed Processes: A Mini-Review. *Ind. Eng. Chem. Res.* **2001,** *40*, 2396-2401.

(21) Lambert, A.; Yeguas, V.; Monard, G.; Ruiz-Lopez, M. F., What Is the Effective Dielectric Constant in a Beta-Cyclodextrin Cavity? Insights from Molecular Dynamics Simulations and Qm/Mm Calculations. *Comput. Theo. Chem.* **2011,** *968*, 71-76.

(22) Sieffert, N.; Wipff, G., Adsorption at the Liquid-Liquid Interface in the Biphasic Rhodium Catalyzed Hydroformylation of Olefins Promoted by Cyclodextrins: A Molecular Dynamics Study. *J. Phys. Chem. B* **2006,** *110*, 4125-4134.

(23) Sieffert, N.; Wipff, G., Importance of Interfacial Adsorption in the Biphasic Hydroformylation of Higher Olefins Promoted by Cyclodextrins: A Molecular Dynamics Study at the Decene/Water Interface. *Chem-Eur J.* **2007,** *13*, 1978-1990.

(24) Raffaini, G.; Ganazzoli, F.; Malpezzi, L.; Fuganti, C.; Fronza, G.; Panzeri, W.; Mele, A., Validating a Strategy for Molecular Dynamics Simulations of Cyclodextrin Inclusion Complexes through Single-Crystal X-Ray and Nmr Experimental Data: A Case Study. *J. Phys. Chem. B* **2009,** *113*, 9110-9122.

(25) Zhang, H. Y.; Feng, W.; Li, C.; Lv, Y. Q.; Tan, T. W., A Model for the Shuttle Motions of Puerarin and Daidzin inside the Cavity of Beta-Cyclodextrin in Aqueous Acetic Acid: Insights from Molecular Dynamics Simulations. *J. Mol. Model.* **2012,** *18*, 221-227.

(26) Zheng, X. Y.; Wang, D.; Shuai, Z. G.; Zhang, X., Molecular Dynamics Simulations of the Supramolecular Assembly between an Azobenzene-Containing Surfactant and Alpha-Cyclodextrin: Role of Photoisomerization. *J. Phys. Chem. B* **2012,** *116*, 823-832.

(27) Jana, M.; Bandyopadhyay, S., Molecular Dynamics Study of Beta-Cyclodextrin-Phenylalanine (1:1) Inclusion Complex in Aqueous Medium. *J. Phys. Chem. B* **2013,** *117*, 9280-9287.

(28) Mathapa, B. G.; Paunov, V. N., Self-Assembly of Cyclodextrin-Oil Inclusion Complexes at the Oil-Water Interface: A Route to Surfactant-Free Emulsions. *J. Mater. Chem. A* **2013,** *1*, 10836-10846.

(29) Hess, B.; Kutzner, C.; van der Spoel, D.; Lindahl, E., Gromacs 4: Algorithms for Highly Efficient, Load-Balanced, and Scalable Molecular Simulation. *J. Chem. Theory Comput.* **2008,** *4*, 435-447.

(30) Lindorff-Larsen, K.; Piana, S.; Palmo, K.; Maragakis, P.; Klepeis, J. L.; Dror, R. O.; Shaw, D. E., Improved Side-Chain Torsion Potentials for the Amber Ff99sb Protein Force Field. *Proteins* **2010,** *78*, 1950-1958.

(31) Silva, A. W. S. d.; Vranken, W. F., Acpype - Antechamber Python Parser Interface. *BMC Resarch Notes* **2012,** *5*, 367-374.

(32) Jakalian, A.; Jack, D. B.; Bayly, C. I., Fast, Efficient Generation of High-Quality Atomic Charges. AM1-BCC Model: II. Parameterization and Validation. *J. Comput. Chem.* **2002,** *23*, 1623-1641.

(33) http://www.yasara.org/autosmiles.htm Automatic Force Field Parameter Assignment in Yasara.

(34) Lague, P.; Pastor, R. W.; Brooks, B. R., Pressure-Based Long-Range Correction for Lennard-Jones Interactions in Molecular Dynamics Simulations: Application to Alkanes and Interfaces. *J. Phys. Chem. B* **2004,** *108*, 363-368.

(35) Jungwirth, P.; Tobias, D. J., Chloride Anion on Aqueous Clusters, at the Air-Water Interface, and in Liquid Water: Solvent Effects on Cl^- Polarizability. *J. Phys. Chem. A* **2002,** *106*, 379.

(36) Vrbka, L.; Mucha, M.; Minofar, B.; Jungwirth, P.; Brown, E. C.; Tobias, D. J., Propensity of Soft Ions for the Air/Water Interface. *Curr. Opin. Colloid Int. Sci.* **2004,** *9*, 67-73.

(37) Lamoureux, G.; Roux, B., Absolute Hydration Free Energy Scale for Alkali and Halide Ions Established from Simulations with a Polarizable Force Field. *J. Phys. Chem. B* **2006,** *110*, 3308-3322.

(38) Chang, T. M.; Dang, L. X., Computational Studies of Liquid Water and Diluted Water in Carbon Tetrachloride. *J. Phys. Chem. A* **2008,** *112*, 1694-1700.

(39) Betzel, C.; Saenger, W.; Hingerty, B. E.; Brown, G. M., Topography of Cyclodextrin Inclusion Complexes .20. Circular and Flip-Flop Hydrogen-Bonding in

Beta-Cyclodextrin Undecahydrate - a Neutron-Diffraction Study. *J. Am. Chem. Soc.* **1984,** *106*, 7545-7557.

(40) Lindner, K.; Saenger, W., Crystal and Molecular-Structure of Cyclohepta-Amylose Dodecahydrate. *Carbohyd. Res.* **1982,** *99*, 103-115.

(41) Steiner, T.; Koellner, G., Crystalline Beta-Cyclodextrin Hydrate at Various Humidities - Fast, Continuous, and Reversible Dehydration Studied by X-Ray-Diffraction. *J. Am. Chem. Soc.* **1994,** *116*, 5122-5128.

(42) Zabel, V.; Saenger, W.; Mason, S. A., Topography of Cyclodextrin Inclusion Complexes .23. Neutron-Diffraction Study of the Hydrogen-Bonding in Beta-Cyclodextrin Undecahydrate at 120-K - from Dynamic Flip-Flops to Static Homodromic Chains. *J. Am. Chem. Soc.* **1986,** *108*, 3664-3673.

(43) Lawtrakul, L.; Viernstein, H.; Wolschann, P., Molecular Dynamics Simulations of Beta-Cyclodextrin in Aqueous Solution. *Int. J. Pharm.* **2003,** *256*, 33-41.

(44) Heine, T.; Santos, H. F.; Patchkovskii, S.; Duarte, H. A., Structure and Dynamics of Beta-Cyclodextrin in Aqueous Solution at the Density-Functional Tight Binding Level. *J. Phys. Chem. A* **2007,** *111*, 5648-5654.

(45) Rodriguez, J.; Rico, D. H.; Domenianni, L.; Laria, D., Confinement of Polar Solvents within Beta-Cyclodextrins. *J. Phys. Chem. B* **2008,** *112*, 7522-7529.

(46) Shikata, T.; Takahashi, R.; Satokawa, Y., Hydration and Dynamic Behavior of Cyclodextrins in Aqueous Solution. *J. Phys. Chem. B* **2007,** *111*, 12239-12247.

(47) Bagchi, B., Water Dynamics in the Hydration Layer around Proteins and Micelles. *Chem. Rev.* **2005,** *105*, 3197-3219.

(48) Laage, D.; Hynes, J. T., A Molecular Jump Mechanism of Water Reorientation. *Science* **2006,** *311*, 832-835.